BMC Microbiology

RESEARCH

Open Access

More powerful dysregulation of *Helicobacter pylori* East Asian-type CagA on intracellular signalings

Xiaofei Ji[1†], Zekun Sun[1†], Hao Wu[1,2†], Jianhui Zhang[1], Shuzhen Liu[1], Xinying Cao[1], Bin Wang[1], Feifan Wang[1], Ying Zhang[1], Boqing Li[1], Jiankai Feng[1] and Huilin Zhao[1*]

Abstract

Background Chronic infection by *Helicobacter pylori* strains expressing cytotoxin-associated gene A (CagA) are the strongest risk factor for gastric cancer. CagA can be classified into East Asian-type and Western-type ($CagA^{E}$ and $CagA^{W}$), with $CagA^{E}$ being more closely associated with gastric cancer. This study aimed to investigate the impact of $CagA^{E}$ on intracellular signaling pathways to explain its high oncogenicity.

Results Mutant *H. pylori* strains expressing either $CagA^{E}$ or $CagA^{W}$ were generated by transforming $CagA^{E/W}$-expression plasmid into CagA-deleted G27 strain ($G27^{\Delta CagA}$). In human gastric epithelial cells (GES-1) infection, $CagA^{E}$ induced more severe cytopathic changes, including higher interleukin-8 (IL-8) secretion, reduced cell viability, more pronounced "hummingbird phenotype" alterations, and increased cell migration and invasion compared to $CagA^{W}$. Transcriptome analysis revealed that $CagA^{E}$ had a stronger effect on the up-regulation of key intracellular processes, including tumor necrosis factor-α (TNF-α) signal pathway via nuclear factor kappa-B (NF-κB), inflammatory response, interferon-γ (IFN-γ) response, hypoxia, ultraviolet (UV) response, and Kirsten Rat Sarcoma Viral Oncogene Homolog (KRAS) signaling. A significant upregulation of hypoxia-related genes was a notable feature of $CagA^{E}$. GES-1 cells infected with $CagA^{E}$ exhibited more severe intracellular hypoxia and higher levels of reactive oxygen species (ROS) than those infected with $CagA^{W}$. Inhibition of hypoxia-inducible factor-1α (HIF-1α), which blocks hypoxia signaling, mitigated $CagA^{E}$-induced cell migration, emphasizing the role of hypoxia in mediating $CagA^{E}$ effects.

Conclusions The study provides transcriptome evidence of CagA-associated intracellular regulation during *H. pylori* infection, demonstrating that $CagA^{E}$ exerts stronger effects on intracellular signaling than $CagA^{W}$. These findings offer insights into the heightened carcinogenic potential of $CagA^{E}$ in *H. pylori*-induced gastric cancer.

Keywords *Helicobacter pylori*, CagA, Transcriptome analysis, Gastric cancer, Hypoxia

[†]Xiaofei Ji, Zekun Sun, Hao Wu contributed equally to this work and share first authorship.

*Correspondence:
Huilin Zhao
zhaohuilin1984@163.com
[1]Binzhou Medical University, Yantai, China
[2]Department of Blood Transfusion, Jining First People's Hospital, Jining, China

Introduction

Helicobacter pylori (*H. pylori*) is a spiral-shaped, microaerophilic Gram-negative bacterium that colonizes the stomach and can cause persistent infection [1, 2]. *H. pylori* infection is associated with various upper gastrointestinal disorders, including chronic gastritis, peptic ulcers, gastric cancer (GC), and gastric mucosa-associated lymphoid tissue lymphoma (MALT). The pathogenicity of *H. pylori* is largely driven by several virulence factors, with cytotoxin-associated gene A (CagA) being one of the most critical in linking infection to the development of GC [3–5].

CagA is encoded by the *cagA* gene located on the *cag* pathogenicity island, found in certain *H. pylori* strains [6–8]. Clinical data show that CagA-positive strains are more likely to cause gastric cancer (GC) than CagA-negative ones [9, 10]. The *cagA* gene encodes a variable C-terminal region containing repeated Glu-Pro-Ile-Tyr-Ala (EPIYA) motifs, which result in a molecular weight ranging from 120 to 145 kDa [7, 11]. Based on flanking sequences, these EPIYA motifs are classified into four types, EPIYA-A, EPIYA-B, EPIYA-C, and EPIYA-D [12, 13]. Geographical evolution has led to distinct combinations of these EPIYA motifs. In East Asian strains (e.g., Japan, Korea, and China), CagA is characterized by a tandem arrangement of EPIYA-A, -B, and -D segments, whereas strains from other regions typically contain EPIYA-A, -B and a variable number (1–4) of EPIYA-C segments [14–17].

Extensive molecular epidemiological studies have shown that individuals infected with East Asian-type CagA ($CagA^E$) strains have a higher risk of developing GC [18, 19]. Transgenic mouse models have demonstrated that $CagA^E$ induces more severe neoplastic lesions than Western-type A ($CagA^W$) [20]. In vitro studies have also shown that $CagA^E$ is more virulent than $CagA^W$ inducing greater IL-8 secretion and more pronounced morphological changes [21, 22]. These findings all suggest that $CagA^E$ is more carcinogenic than $CagA^W$, although the underlying mechanisms remain unclear.

During *H. pylori* infection, CagA is delivered into gastric epithelial cells via the bacterial type IV secretion system (T4SS), which is also encoded by *cag* pathogenicity island [8, 23, 24]. Once inside the host cell, CagA binds to the inner leaflet of the plasma membrane through its N-terminal region. The C-terminal EPIYA motifs undergo phosphorylation at tyrosine residues by host kinases c-Src and c-Abl [25–27]. Phosphorylated or non-phosphorylated CagA interacts with various intracellular signaling through its EPIYA motifs, hijacking host cell signaling pathways and contributing to carcinogenesis [8]. A key binding site for the EPIYA motif is the SH2 domain, found in several host proteins, including SH2 domain-containing PTPase2 (SHP2), SH2 domain-containing PTPase1 (SHP1), C-terminal SRC kinase (CSK), growth factor receptor-bound protein 2 (Grb2), growth factor receptor-bound protein 7 (Grb7), phosphatidylinositol-3 kinase (PI-3 kinase) [28–31]. Due to variations in the EPIYA-C and EPIYA-D sequences, $CagA^E$ and $CagA^W$ may interact differently with these host proteins, leading to distinct pathogenic outcomes. Hayashi et al. demonstrated that the EPIYA-D segment of $CagA^E$ actives SHP2 more strongly than the EPIYA-C segment contributing to greater "hummingbird phenotype" formation in cells injected with $CagA^E$ [32]. However, the broader intracellular behaviors of $CagA^E$ and $CagA^W$ remain unclear, complicating our understanding of the differences in their pathogenicity.

Previous studies have examined the global transcriptional responses of gastric epithelial cells to *H. pylori* and CagA using DNA microarrays and RNA-seq [33–36]. These studies have gradually uncovered the complex interactions between *H. pylori* infection (and CagA) and host cells, advancing our understanding of CagA-induced carcinogenesis. However, no transcriptomic studies have specifically focused on the different subtypes of CagA.

In this study, we constructed two *H. pylori* mutant strains with identical genetic backgrounds, each expressing either $CagA^E$ or $CagA^W$, to infect gastric epithelial cells. We then compared the transcriptional profiles and phenotypic outcomes of these infected cells to better understand the differential roles of $CagA^E$ and $CagA^W$ in *H. pylori* pathogenesis.

Materials and methods

Bacterial strains, plasmids and primers

Bacterial strains, plasmids, and primers used in this study are listed in Table 1. *H. pylori* strains 26,695 and SHCH-30, encoding $CagA^W$ and $CagA^E$ respectively, were from the repository of our lab and cultured routinely under microaerophilic atmosphere (85% N_2, 10% CO_2, 5% O_2) at 37 °C. Serum plates supplemented with kanamycin (15 mg/L) or chloramphenicol (10 mg/L) were used for selection of *H. pylori* mutant strains. *E. coli* strains were routinely cultured and used for plasmid cloning, and chloramphenicol (30 mg/L) or ampicillin (100 mg/L) was added when needed.

Construction of CagA mutants

H. pylori strain G27 was used as starter to construct mutant strains containing $CagA^E$ or $CagA^W$. Firstly, the original *cagA* gene in G27 was deleted by homologous recombination knockout as described previously [37]. Gene-targeting cassette was constructed on vector pSJHK4 by inserting upstream and downstream homologous arms, which were amplified with primers G27-507-arm1-1, G27-507-arm1-2 and G27-507-arm2-1, G27-507-arm2-2, respectively. The resultant

Table 1 Strains, plasmids and PCR primers used in this study

Strain or plasmid	Description	Reference or source
Strains		
H. pylori 26,695	*H. pylori* wild strain containing Western CagA	
H. pylori SHCH-30	*H. pylori* wild strain containing East Asian CagA	
H. pylori G27	*H. pylori* wild strain containing Western CagA	
H. pylori G27$^{\Delta CagA}$	*H. pylori* G27, *cagA* knockout, km^r	This study
H. pylori G27^{CagAW}	*H. pylori* G27$^{\Delta CagA}$, Western CagA knockin, km^r, cm^r	This study
H. pylori G27^{CagAE}	*H. pylori* G27$^{\Delta CagA}$, East Asian CagA knockin, km^r, cm^r	This study
E. coli-DH5α	Strain used for gene cloning	Tiangen
Plasmids		
pSJHK4	Gene-targeting template plasmid, Ap^r (km^r)	[37]
pSJHK4-CagA	A *cagA* targeted vector, Ap^r (km^r, cm^r)	This study
pCHFHP	*H. pylori-E. coli* shuttle plasmid, Ap^r (cm^r)	This study
Primers		
G27-507-arm1-1	5′-GACCAGGGATCCAGTCTCAGTGACGCCTGTTGCA-3′	This study
G27-507-arm1-2	5′-GGCCACCATATGATTATTGATAAATTGCTGCGGGTT-3′	This study
G27-507-arm2-1	5′-GCGTCCCTCGAGTTGAACAATGCTGTAAAAGA-3′	This study
G27-507-arm2-2	5′-CGATGCTAGTCTAGAATATTTGCAGCAAAAAT-3′	This study
507-test-1	5′-GTCATTTGCTGACCCATACGA-3′	This study
507-test-2	5′-GGCGTGATTGAGCCAAGCATT-3′	This study
Km-tset-1	5′-TGCCTCGTCTTGGAGTTCATTC-3′	This study
Km-tset-2	5′-GTTGGCTACCCGTGATATTGCT-3′	This study

Ap ampicillin, *Km* kanamycin, *Cm* chloramphenicol

plasmid pSJHK4-CagA was transformed into *H. pylori* by natural transformation, to generate CagA deleted strain (G27$^{\Delta CagA}$). Diagnostic PCR was performed to confirm the deletion of CagA with primers 507-test-1, Km-tset-1 and Km-tset-2, 507-test-2. The primers were indicated in Fig. 1A and sequences were listed in Table 1.

The coding sequence of CagA^W or CagA^E was amplified from the genome of *H. pylori* 26,695 or SHCH-30, and subsequently ligated into *H. pylori-E. coli* shuttle plasmid pCHFHP, to produce CagA-expression plasmid (pCHFHP-CagA), which was shown in Fig. 1C. These plasmids were transformed into G27$^{\Delta CagA}$ also by natural transformation for screening G27^{CagAW} and G27^{CagAE} mutants.

Cell culture and infection

Human immortalized gastric epithelial GES-1 (Beyotime Biotechnology, C6268, China) cultured in Dulbecco's Modified Eagle Medium (DMEM) (Macgene, CM10017, China) containing 10% fetal bovine serum (FBS) (Gibco, FSS500, USA) was used as the recipient cell for *H. pylori* infection. Mid-exponential-phase *H. pylori* cells were suspended in PBS (Meilunbio, MA0015, China), and added into cell cultures at a multiplicity of infection (MOI) of 100:1. After incubating for 4 h, cells were collected for RNA extracting and phenotypic testing. The morphology of cells was observed by using a microscope at ×20 magnification and *H. pylori*-induced "hummingbird phenotype" elongation cells were counted.

Cultivation of mouse stomach organoids and establishment of infection

The 6-week-old male C57BL/6 mice were purchased from Jinan Pengyue Laboratory Animal Breeding Co. After a one-week adaptation period, the mice were euthanized by cervical dislocation. Glandular cells from antrum and corpus were isolated and cultured as the procedures described by Mahe et al. and Schumacher et al. [38, 39]. In a nutshell, the stomach of approximately 1 cm^2 was firstly cut into small pieces and washed in cold Ca^{2+}/Mg^{2+}-free D-PBS (Procell, PB180329, China) until the supernatant was clear. Pieces were enzymatically digested by 1 mg/mL of collagenase and 0.5 mg/mL of hyaluronidase in 5 mL Advanced DMEM/F12 (Gibco, 12634010, USA) medium for 30 min. After repeated washing and centrifugation to remove enzymes, the gastric glandular cells were suspended and seeded into Matrigel (R&D system, 3533-005-02, USA) and maintained in medium containing: 100 ng/mL of Wnt3A (Peprotech, 315−20, USA), 100 ng/mL of Noggin (R&D system, 1967-NG, USA), 500 ng/mL of R-Spondin-1 (Peprotech, 315−32, USA), Glutamax-I (1×) (Gibco, 35050061, USA), 1% of Penicillin/streptomycin (Gibco, 15070063, USA),100 ng/mL of FGF-10 (R&D system, 6224-FG, USA), 50 ng/mL of EGF (R&D system, 2028-EG, USA), 1×B27 (Gibco, 17504044, USA), 10 nM of Gastrin-1 (Tocris Bioscience, 3006, UK), 1 mM of N-Acetylcysteine (Tocris Bioscience, 5619, UK) during the whole cultivation and 10 μM of Y-27,632 (Tocris Bioscience, 1254, UK) for only the first 2 days. The medium was replaced three times a week [40, 41].

One-week-old organoids were harvested from matrigel and transferred to planar cultures as the methods described by Schlaermann et al. [42]. *H. pylori* was added in the medium at an MOI of 100:1 for the infection.

Cell vitality assay

Cell Counting Kit-8 (CCK-8, Meilun Biotechnology Co., Ltd, Dalian, China) was used to measure the cell vitality. GES-1 cells were seeded into 96-well plates at a density

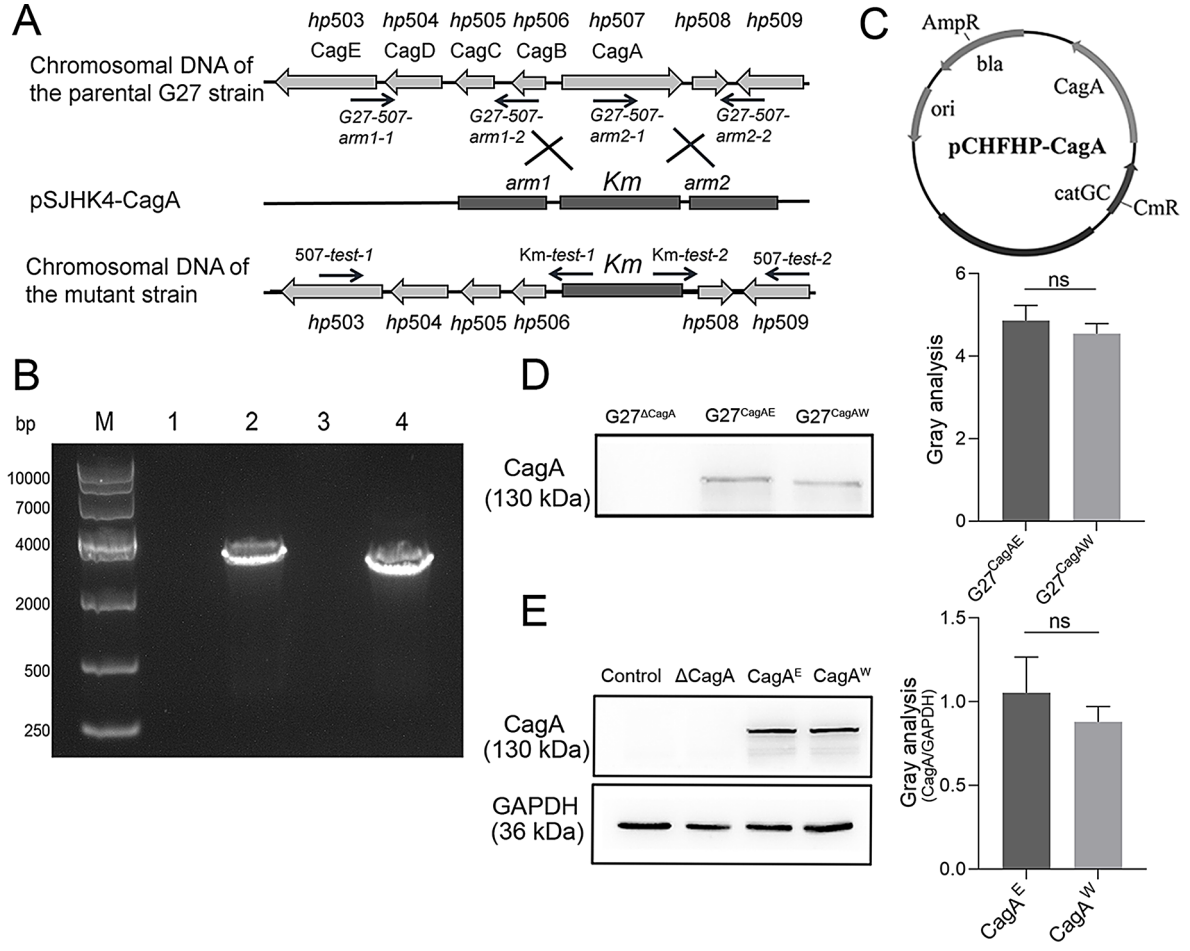

Fig. 1 Construction of G27$^{\Delta CagA}$, G27^{CagAE} and G27^{CagAW} mutants on the basis of *H. pylori* G27 strain. (**A**) Schematic representation of the deletion of CagA. Two homologous arms (arm1 and arm2) for targeting CagA with a gene number of *hp507* were amplified from the genome of *H. pylori* G27 with two sets of primers G27-507-arm1-1/G27-507-arm1-2 and G27-507-arm2-1/G27-507-arm2-2, and ligated into the template plasmid pSJHK4. The gene-targeting plasmid pSJHK4-CagA was transformed into *H. pylori* by natural transformation, and transformants were selected by kanamycin resistance. Black boxes indicate upstream and downstream homologous arms, respectively. Arrowheads indicate the arrangements and orientations of genes. (**B**) Verification of genetic recombination by diagnostic PCR. *Lane* M, DNA molecular weight standard (DL10000); *Lane* 1 and 2, PCR products amplified using primers 507-test-1 and Km-test-1 from wild type of *H. pylori* (WT) and the mutant; *Lane* 3 and 4, PCR products amplified using primers 507-test-2 and Km-test-2 from WT and mutant. (**C**) Schematic representations of CagA-expression shuttle plasmid pCHFHP-CagA. (**D**) Immunoblotting of CagA in *H. pylori* WT and mutant strains. G27$^{\Delta CagA}$, G27^{CagAE} and G27^{CagAW} represent CagA deleted, CagA^{E} containing and CagA^{W} containing mutant strains, respectively. (**E**) Immunoblotting of CagA in the cell lysate of GES-1 cells infected with *H. pylori* WT and mutant strains. The groups of ΔCagA, CagA^{E}, CagA^{W} and Control respectively represent GES-1 cells infected with G27$^{\Delta CagA}$, G27^{CagAE}, G27^{CagAW} and without infection. GAPDH was used as an internal control. ns, no significance

of 4×10^3 cells/well, and infected with *H. pylori* for 4 h. Then, the supernatants were discarded and the cells were washed three times with PBS. DMEM (Macgene) containing 10% of CCK-8 reagent was added into 96-well plates for another 2 h's incubation at 37 °C and the optical density (OD) of the mixture was detected at a wavelength of 450 nm by using SpectraMax Plus384 (Molecular Devices, Silicon Valley, USA).

Transwell assay

Transwell chambers (Corning, New York, USA) with or without Matrigel (Abwbio, Shanghai, China) were used to determine cells' invasion or migration. After starved in serum-free medium for 12 h, the test cells were seeded into the upper chamber at a density of 5×10^4/well. 600 μL of culture medium containing 20% FBS was added into the lower chambers, serving as a chemoattractant. After 48 h incubation, the migrated or invaded cells on the lower surface of the chamber filters were fixed with 4% paraformaldehyde, stained with 0.1% crystal violet and counted under the microscope (Olympus).

Measurement of IL-8 secretion

The supernatant of infected cell culture was collected for IL-8 amount determination using a Human IL-8 ELISA Kit (Elabscience Biotechnology Co., Ltd, Wuhan, China) according to the manufacturer's instructions. The absorption at 450 nm was also read by SpectraMax Plus384

(Molecular Devices), and the concentration of IL-8 was calculated based on the standard curve.

Hypoxia analysis and intracellular ROS detection

The hypoxia level of GES-1 cells was analyzed by confocal scanning microscopy (Zeiss LSM880 Airyscan, Oberkochen, Germany) after treated with the ROS-ID Hypoxia/Oxidative stress detection kit (Enzo Life Sciences, Farmingdale, USA) according to the manufacturer's instructions (for fluorescence signal of hypoxia, excitation filter: 420 nm, emission filter: 600–700 nm).

RNA extraction and sequence analysis

After 4 hours' incubation with *H. pylori* strains, $G27^{CagAW}$ or $G27^{CagAE}$, GES-1 cells were washed twice with PBS to remove non-adherent bacteria. Total RNA was extracted from GES-1 cells by using the Trizol reagent (Invitrogen, Grand Island, USA) with conventional procedure. Residual genomic DNA in RNA samples were removed by incubation with DNA-free DNase I (Ambion, Austin, USA) at 37 °C for 30 min. The quantity and purity of the harvested RNA were determined by using Qsep 100 (Bioptic, Taiwan, China) and RNA 1000 Nano LabChip Kit (Agilent, Santa Clara, CA, USA). The samples with quality number (RQN) greater than 7 was sequentially processed with mRNA capture, RNA fragmentation, cDNA synthesis, ending-repair, dA-tailing, adapter ligation and magnetic bead purification and separation. The cDNA libraries were generated using the VAHTS Universal V8 RNA-seq Library Prep Kit for Illumina (Vazyme Biotech Co., Ltd, Nanjing, China) in accordance with the manufacturer's protocol. Finally, libraries fragment distribution were profiled in Qsep 100 and sequenced on NovaSeq 6000 platform using paired-end RNA-seq approach (Novogene, Beijing, China).

Transcriptome analysis

Fastp software (version 0.23.2) was firstly employed to process the raw reads from RNA-seq with default parameters to remove unqualified reads [43]. The valid data generated was aligned to the reference genome of Homo sapiens GRCh38 p.14 using subjunc aligner. The gene-sample count table was generated by featureCounts [44]. R software (version 4.2.1) and the package DESeq2 (version 4.2.1) were adopted to analyze mRNAs and genes expressed differentially [45], and variance stabilizing transformation (VST) [46] was performed to normalize the read counts. The influences of *H. pylori* infection on GES-1 cells were explored by gene set enrichment analysis (GSEA) against Molecular Signatures Database (MSigDB, version 7.5.1) using clusterProfiler packages (version 4.4.2) [47, 48].

Quantitative real-time PCR

To verify the differential expression genes screened from transcriptome analysis, qRT-PCR was performed using an ABI Prism 7500 Detection System (Applied Biosystems, Foster City, USA) with 2×SYBR Green qPCR Mix (Sparkjade, Shandong, China) as the fluorescent detection dye. First-strand cDNA was synthesized from 1 μg of total mRNA, and applied as the template for qRT-PCR with gene-specific primers. The PCR thermal cycling conditions for all reactions were 94 °C for 3 min, followed by 40 cycles of 94 °C for 10 s and 60 °C for 34 s. All reactions were performed for three biological replicates, and the data for each sample were calculated relatively to the levels of reference gene (GAPDH) by using $2^{-\Delta\Delta CT}$ method [49, 50]. The primer sequences were listed in Supplementary Table 1.

Western blotting

Total protein of infected GES-1 cells was extracted in RIPA lysis buffer (Solarbio, Beijing, China) and quantified by bicinchoninic acid (BCA) detection kit (Beyotime, Shanghai, China). After separated by SDS-PAGE, proteins were electrotransfered to a PVDF membrane and sequentially incubated with primary and secondary antibodies. Protein blots on PVDF membranes were then colorized by an enhanced chemiluminescence reagent and imaged by Tanon 5200 Multi chemiluminescent imaging system (Shanghai, China). Antibodies used in this study include anti-CagA (Santa Cruz Biotechnology, Dallas, USA), anti-GAPDH (Proteintech, Wuhan, China) as primary antibody and anti-mouse IgG-HRP (Proteintech) as secondary antibodies.

Statistics

Statistical analysis was performed by GraphPad Prism software version 9. Results are showed as means ± standard error of the means (SEM). Tests in comparison between groups were analyzed to get *P* value, and differences were considered statistically significant when when $P<0.05$.

Results

Construction of $CagA^{E}$ or $CagA^{W}$ harboring mutant strains

To investigate the distinct roles of CagA subtypes in *H. pylori* pathogenesis, we generated *H. pylori* G27 strains expressing either $CagA^{E}$ or $CagA^{W}$. First, the endogenous CagA gene in *H. pylori* G27 was deleted to create a CagA knockout ($G27^{\Delta CagA}$) mutant (Fig. 1A). This was achieved by transforming *H. pylori* with the plasmid pSJHK4-CagA, replacing the *cagA* gene with a selection marker kanamycin resistance gene (*Km*) via double-crossover homologous recombination. Transformants were selected on kanamycin and confirmed by diagnostic PCR. As shown in Fig. 1B, two specific amplicons

were observed in the mutant strain, corresponding to the regions flanking the deleted *cagA* gene, which were absent in the wild-type strain. This confirmed the successful generation of the $G27^{\Delta CagA}$ strain.

Next, we transformed the $G27^{CagA}$ strain with plasmids expressing either $CagA^{E}$ or $CagA^{W}$, resulting in the $G27^{CagAE}$ and $G27^{CagAW}$ strains, respectively (Fig. 1C). Western blot analysis confirmed the expression of CagA in both mutant strains, with no detectable CagA in the specific $G27^{\Delta CagA}$ strain (Fig. 1D). The expression levels of $CagA^{E}$ and $CagA^{W}$ were similar, indicating that both subtypes were successfully expressed at comparable levels.

Since CagA is translocated into host cells during *H. pylori* infection, we also assessed the intracellular levels of CagA in infected GES-1 cells (Fig. 1E). CagA was detected in cells infected with either $G27^{CagAW}$ or $G27^{CagAE}$, with no significant difference in the amount of CagA between the two strains. As expected, no CagA was detected in cells infected with $G27^{\Delta CagA}$. These results confirmed that the genetic manipulations did not impair the translocation of CagA into host cells. Given the similar expression and translocation levels of CagA $G27^{CagAW}$ and $G27^{CagAE}$, these strains are suitable for comparing the pathogenic differences between the two CagA subtypes.

Phenotypic identification of GES-1 cells infected by different CagA mutants

To investigate the pathogenic effects of different CagA subtypes ($CagA^{E}$ and $CagA^{W}$), GES-1 cells were infected with the *H. pylori* strains $G27^{\Delta CagA}$, $G27^{CagAW}$, and $G27^{CagAE}$. Various phenotypic changes were assessed, including cell morphology, viability, IL-8 secretion, cell migration, and invasion. The infection groups were abbreviated as $CagA^{E}$, $CagA^{W}$ and ΔCagA, respectively, while uninfected GES-1 served as the control.

Previous studies have shown that CagA can induce cytoskeletal rearrangement in host cells, resulting in a distinct "hummingbird phenotype", characterized by an elongated shape with a length-to-width ratio greater than 2:1 [51]. In our study, significant numbers of cells with this special phenotype were observed in both $CagA^{E}$ and $CagA^{W}$ groups, with more elongated cells in the $CagA^{E}$ compared to the $CagA^{W}$ and ΔCagA groups (Fig. 2A). Quantitative analysis revealed that 24.05±0.68% of cells in the $CagA^{E}$ group exhibited the hummingbird phenotype, compared to 15.08±1.02% in the $CagA^{W}$ group, consistent with previous findings that $CagA^{E}$ induces more pronounced morphological changes than $CagA^{W}$ [52].

Cell viability was also assessed, and the results are presented in Fig. 2B. *H. pylori* infection led to a significant reduction in cell viability across all infected groups, regardless of CagA expression. However, CagA-positive strains, particularly $CagA^{E}$, caused a greater decrease in viability than CagA-negative strains, indicating that CagA contributes to cell damage and that $CagA^{E}$ is more cytotoxic than $CagA^{W}$.

As shown in Fig. 2C, H. *pylori* infection significantly increased IL-8 secretion in GES-1 cells, with CagA-positive strains inducing higher levels than the ΔCagA group, consistent with previous study [53]. Specifically, the $CagA^{E}$ group secreted 117.64±1.79 pg/mL of IL-8, compared to 70.46±0.99 pg/mL in the $CagA^{W}$ group and 28.21±2.35 pg/mL in the ΔCagA group. These findings suggest that $CagA^{E}$ triggers a stronger inflammatory response during *H. pylori* infection.

Transwell assays were conducted to evaluate cell migration and invasion (Fig. 2D and E). Infection with CagA-positive *H. pylori* strains enhanced migration and invasion of GES-1 cells, with $CagA^{E}$ exerting a more potent effect than $CagA^{W}$.

RNA transcription analysis of GES-1 cells infected by different *H. pylori* mutants

The transcriptional profiles of GES-1 cells infected with different *H. pylori* strains, expressing distinct types of CagA were analyzed (Fig. 3A). A total of 762,023,558 original reads were obtained from 19 RNA samples (4 independent samples from the ΔCagA group and 5 from each of the other groups). After filtering, 505,980,216 clean reads were retained. The RNA-Seq data has been deposited in the NCBI-SRA with accession number PRJNA1070825. Principal component analysis (PCA) revealed a clear separation among the transcriptomes of cells infected by $G27^{CagAE}$, $G27^{CagAW}$, $G27^{\Delta CagA}$, and the control (uninfected cells), with a total variance of 82.5% explained by two axes (PC1=80%, PC2=2.5%) (Fig. 3B).

Gene Set Enrichment Analysis (GSEA) was used to identify altered hallmark gene sets, using cut-off values of |Normalized Enrichment Score| (|NES|)>1, Nominal p-value (NOM.p.val)<0.05 and False Discovery Rate q-value (FDR.q.val)<0.25. Compared to the control, 16 gene sets were significantly altered in the $CagA^{E}$ group, 14 in the $CagA^{W}$ group, and 10 in the ΔCagA group (Fig. 3C-E, Supplementary Tables 2–4). Eight gene sets were shared across all infected groups, including the TNF-α signaling via NF-κB, hypoxia, inflammatory response, IFN-γ response, IL-6/JAK/STAT3 signaling, allograft rejection, IL-2-STAT5 signaling, and UV response pathways. These gene sets are predominantly associated with inflammation and immune response, indicating the main host response to *H. pylori* infection. The NES and FDR.q.val. values showed higher expression levels of these inflammatory genes in the $CagA^{E}$ group compared to the $CagA^{W}$ group (Fig. 3C-E, Supplementary Tables 2–4), consistent with phenotypic assays that demonstrated more severe cellular damage in the

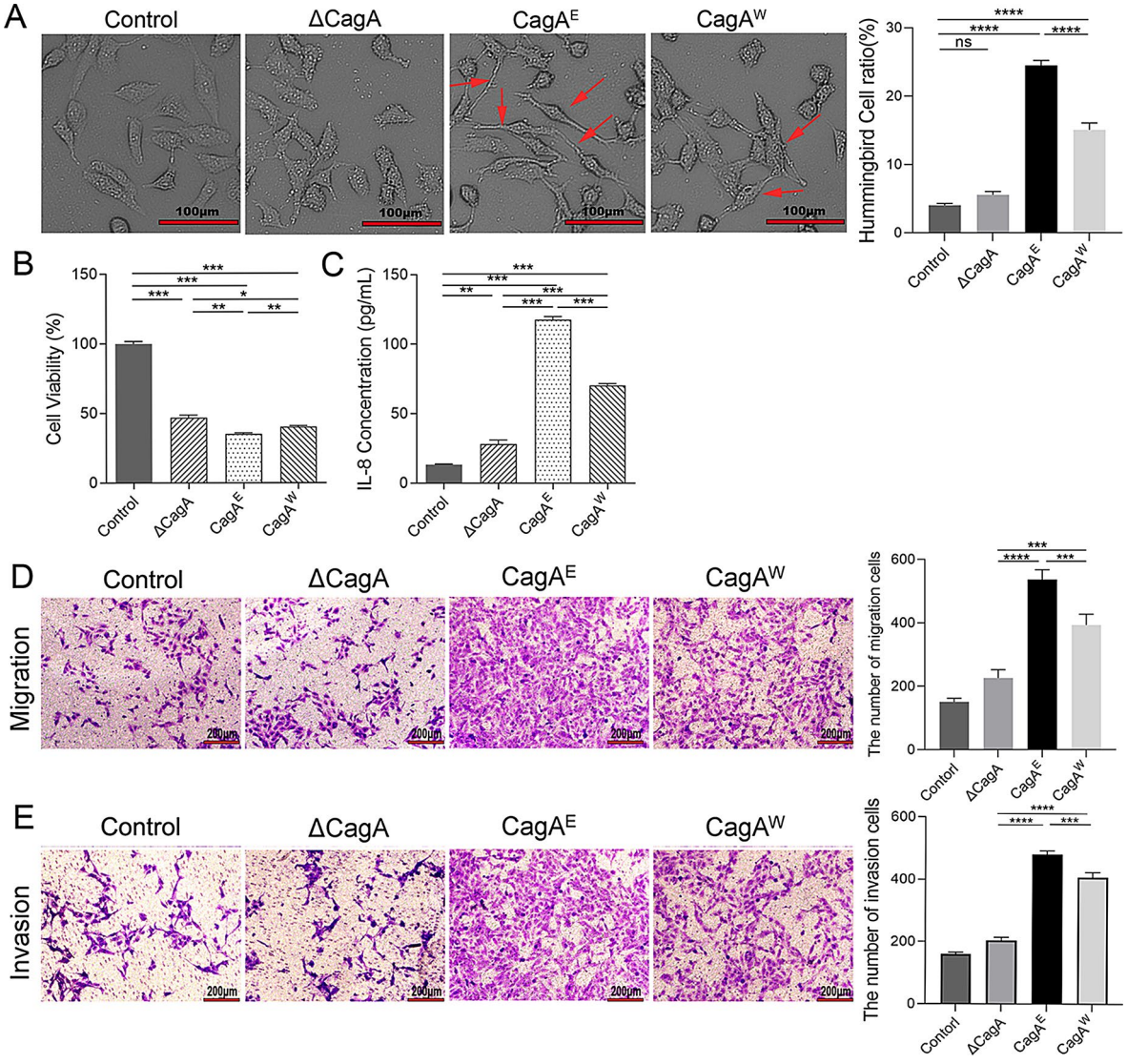

Fig. 2 Phenotypic identification of GES-1 cells infected with different *H. pylori* mutant strains. (**A**) The "hummingbird phenotype" alteration, (**B**) Cell viability, (**C**) IL-8 secretion, (**D**) Migration and (**E**) invasion. Left, Representative images; Right, statistical data. Cells with "hummingbird phenotype" were indicated by red arrows. Error bars represent means ± SEM., **P* < 0.05, ***P* < 0.01, ****P* < 0.001 and *****P* < 0.0001

$CagA^E$-infected cells. Additionally, both $CagA^E$ and $CagA^W$ groups exhibited co-enrichment in pathways related to apoptosis, KRAS signaling up, Epithelial-to-mesenchymal transition (EMT), and complement activation, underscoring CagA involvement in these processes. Notably, the enrichment of these pathways was higher in the $CagA^E$ group compared to $CagA^W$. $CagA^E$ also uniquely enriched several additional gene sets, including mTORC1 signaling, the Reactive Oxygen Species (ROS) pathway, Unfolded Protein Response, and the P53 pathway.

To further explore the regulatory differences between $CagA^E$ and $CagA^W$, a direct comparison with the ΔCagA group was performed. Three up-regulated gene sets - TNF-α signaling via NF-κB, IFN-γ response, and inflammatory response- were shared between the $CagA^E$/ΔCagA group and $CagA^W$/ΔCagA comparisons, indicating their close association with CagA activity (Fig. 3F-G, Supplementary Tables 5–6). However, pathways related to hypoxia, UV response, and KRAS signaling were only enriched in the $CagA^E$/ΔCagA group comparison, highlighting the distinct regulatory effects of $CagA^E$. Interestingly, when directly comparing $CagA^E$ and $CagA^W$, the hypoxia pathway was the only gene set significantly up-regulated in the $CagA^E$ group (Fig. 3H, Supplementary Table 7). These findings suggest that while both CagA subtypes activate common inflammatory and immune pathways, $CagA^E$ exerts additional regulatory effects, particularly through the hypoxia pathway, contributing to its enhanced pathogenicity.

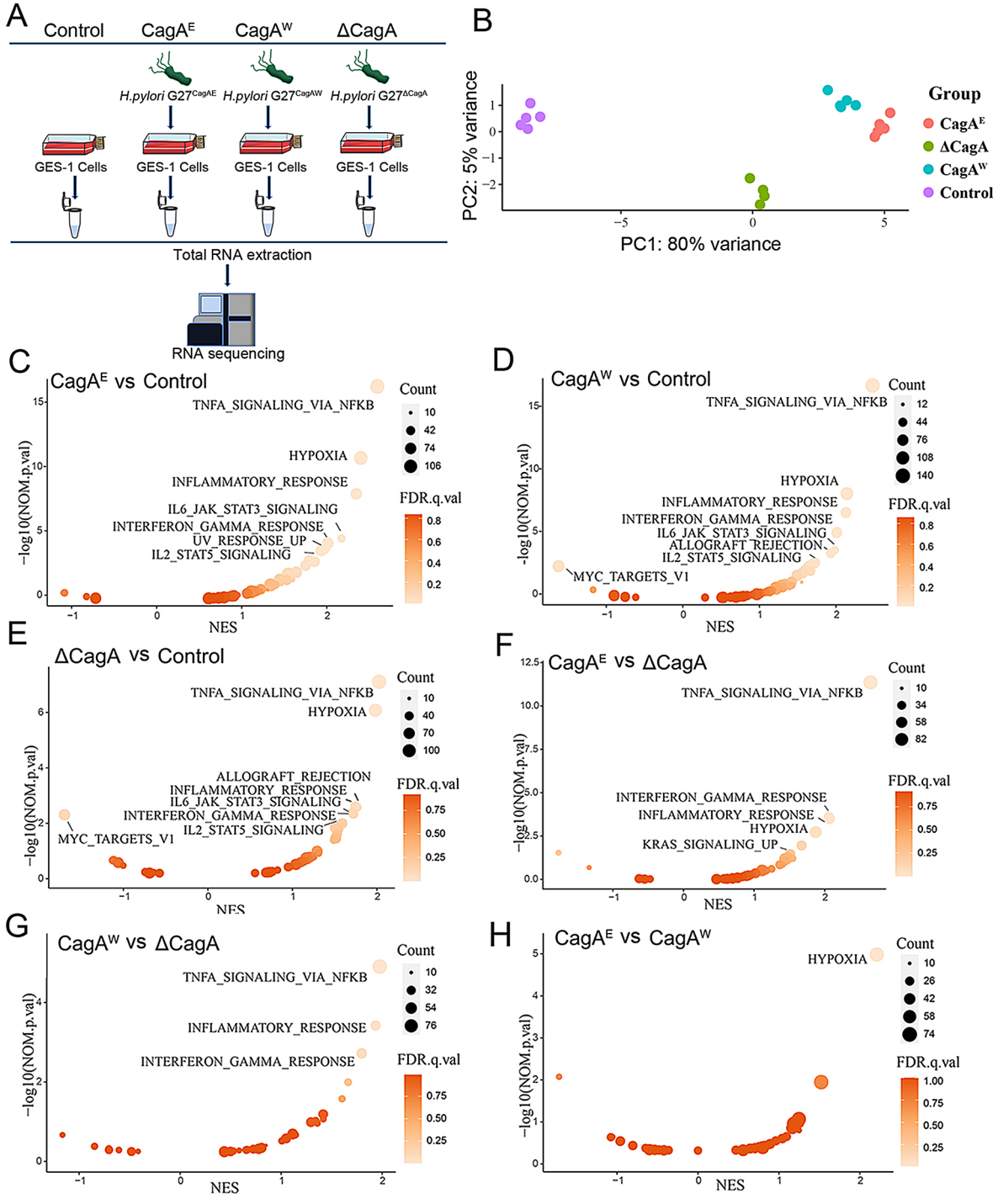

Fig. 3 Identification of significantly differential gene sets in *H. pylori* infected GES-1 cells from RNA sequencing results. (**A**) Schematic view of the experimental workflow for transcriptome sequencing in GES-1 cells infected by *H. pylori* mutants. (**B**) PCA analysis revealing significant differences in transcriptome levels among four groups. Purple, green, red and blue dots respectively represent Control, ΔCagA, CagA^{E} and CagA^{W} group clusters. (**C**-**H**) Scatter diagrams of differential gene sets with a cutoff of |NES| > 1, NOM.p.val < 0.05 and FDR.q.val < 0.25. **C**, CagA^{E} vs. Control group; **D**, CagA^{W} vs. Control group; **E**, ΔCagA vs. Control group; **F**, CagA^{E} vs. ΔCagA group; **G**, CagA^{W} vs. ΔCagA group; **H**, CagA^{E} vs. CagA^{W} group. X-axis refers to the value of NES; Y-axis refers to the value of -log10 (NOM.p.val); The size and color of the bubbles represent the counts of genes enriched in gene sets and FDR.q.val, respectively

Verification of differentially expressed gene sets

To validate the differential gene expression identified in the transcriptome analysis, we focused on the three significantly up-regulated gene sets closely related to CagA, identified in comparisons between the $CagA^{E/W}$ and ΔCagA groups. TNF-α signaling via NF-κB, inflammatory response, and IFN-γ response. The significantly differentially expressed (SDE) genes in these processes are listed in Supplementary Tables 5–6. From these gene sets, six genes showing the most pronounced differences - INHBA, TNFRSF9, IL-6, SOD2, CXCL8, and TRAF1 - were selected as representative markers. A heat map of these genes is shown in Fig. 4A. The qRT-PCR results demonstrated that the transcription levels of these genes were up-regulated in GES-1 cells after 4 hours' post-infection with CagA-positive *H. pylori* (Fig. 4B), with the effect being most pronounced in the presence of $CagA^{E}$. To further investigate these expression changes in a more physiologically relevant context, we used mouse-derived stomach organoids to simulate in vivo infection. As shown in Fig. 4C, the expression of INHBA, TNFRSF9, and IL-6 was significantly increased following infection, with $CagA^{E}$ exhibiting a stronger induction effect than $CagA^{W}$, consistent with the results from the in vitro GES-1 cell infection experiments. These findings confirmed that the TNF-α signaling via NF-κB, IFN-γ response, and Inflammatory Response pathways are closely associated with CagA activity and that $CagA^{E}$ exerts a more potent regulatory effect on these pathways than $CagA^{W}$.

In addition, the hypoxia gene set was the only one significantly different between the $CagA^{E}$ and $CagA^{W}$ groups, based on transcriptome comparisons. The enriched genes in this set are listed in Supplementary Table 7. To verify their transcriptional regulation, IGFBP3, STC1, EFNA3 and EFNA1 were selected for further analysis in *H. pylori*-infected cells and stomach organoids. The heat map of these genes is shown in Fig. 5A, with corresponding qRT-PCR results in Fig. 5B and C. As expected, the transcription levels of these genes were higher in the $CagA^{E}$ group compared to the $CagA^{W}$ group, both in infected GES-1 cells and in mouse-derived stomach organoids. These results confirmed the stronger regulation of the hypoxia gene set by $CagA^{E}$ compared to $CagA^{W}$, highlighting hypoxia as a key differential pathway in the intracellular regulation by CagA.

$CagA^{E}$ caused more severe hypoxia enhancing the migration of infected GES-1 cells

The transcriptomic analysis highlighted the up-regulation of the hypoxia gene set as a key feature of $CagA^{E}$-mediated regulation. This prompted us to investigate whether $CagA^{E}$ plays a more active role in driving intracellular hypoxia. To assess the hypoxic response in infected cells, we used a ROS-ID hypoxia/oxidative stress detection kit (Enzo Life Sciences). This kit employs a red fluorescent dye that responds to nitroreductase activity in hypoxic cells by converting the nitro groups to hydroxylamine (NHOH) and amino (NH_2), thereby releasing the fluorescent signal. As shown in Fig. 6A, red fluorescence was notably increased in *H. pylori*-infected GES-1 cells, with the $CagA^{E}$-positive *H. pylori* group exhibiting the highest fluorescence intensity, indicating a more pronounced hypoxic response. Reactive Oxygen Species (ROS) production is a critical marker of intracellular hypoxia and is closely associated with *H. pylori* infection. Using the oxidative stress detection reagent, we stained cells for total ROS, revealing increased green fluorescence in infected GES-1 cells (Fig. 6B). The highest ROS levels were observed in the $CagA^{E}$ group, further supporting that $CagA^{E}$ induces a stronger hypoxic and oxidative stress response compared to $CagA^{W}$. These findings suggest that $CagA^{E}$ is more potent in promoting both hypoxia and ROS production in infected cells.

Hypoxia has been linked to enhanced cell migration and invasion [54]. We hypothesized that the more severe hypoxia induced by $CagA^{E}$ could contribute to greater cell migration and invasion. To test this, we blocked hypoxic signaling to evaluate changes in CagA-induced cell migration. Hypoxia-inducible factor (HIF)-1α, a key regulator of the hypoxic response, was inhibited using LW6, a compound that promotes HIF-1α degradation. As shown in Fig. 6C, inhibition of HIF-1α significantly reduced cell migration in both $CagA^{E}$ and $CagA^{W}$-infected cells, with a 33% decrease in the $CagA^{E}$ group and a 28% decrease in the $CagA^{W}$ group. These results confirm that hypoxia plays a critical role in $CagA^{E}$-induced enhanced cell migration and imply that inhibiting hypoxia could counteract the neoplastic transformation driven by $CagA^{E}$ during *H. pylori* infection.

Discussion

Several in vivo and in vitro studies have demonstrated the strong pathogenic effects of $CagA^{E}$. Miura et al. reported that transgenic mice expressing $CagA^{E}$ developed more severe neoplastic lesions than those expressing $CagA^{W}$ [20]. In cell infection models, $CagA^{E}$-positive strains showed greater inhibition of gap junction intercellular communication in GES-1 cells [55] and induced more IL-8 secretion in co-cultured AGS cells [21]. Fu HY et al. also found that $CagA^{E}$ more actively promoted cell growth than $CagA^{W}$ [56]. Consistent with these findings, our study revealed that $CagA^{E}$ induces a higher degree of phenotypic changes in infected GES-1 cells, including elevated IL-8 secretion, decreased cell viability, a greater occurrence of the "hummingbird phenotype", and increased cell migration and invasion. Despite growing

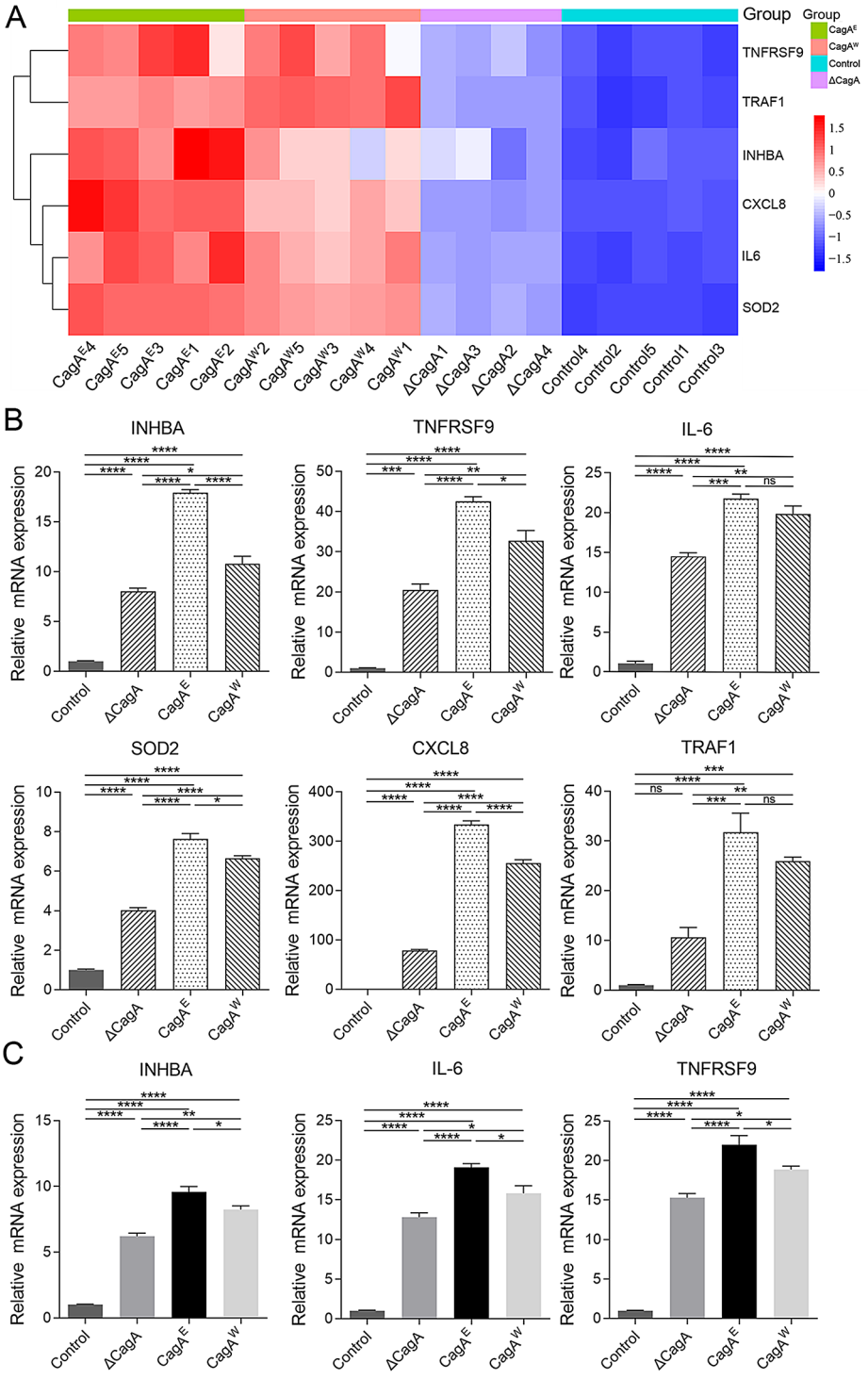

Fig. 4 Validation of the significantly differentially expressed genes under infections by CagA$^{E/W}$ harboring strains and CagA deleted strain. (**A**) The heatmap shows the significantly upregulated mRNAs. Determination of gene's expression in *H. pylori*-infected cells (**B**) and stomach organoids (**C**) was performed by qRT-PCR. GAPDH was selected as an internal control for relative quantification. *$P < 0.05$, **$P < 0.01$, ***$P < 0.001$ and ****$P < 0.0001$

evidence of the heightened cytotoxicity of CagA^{E}, the underlying mechanisms remain poorly understood.

CagA is delivered into host gastric epithelial cells via *H. pylori*'s type IV secretion system, where it modifies intracellular signaling [31, 57]. While many studies have investigated the regulatory effects of CagA^{W} on these signals, few have explored the differences between CagA^{E} and CagA^{W}. Fu HY et al. reported that CagA^{E} has a

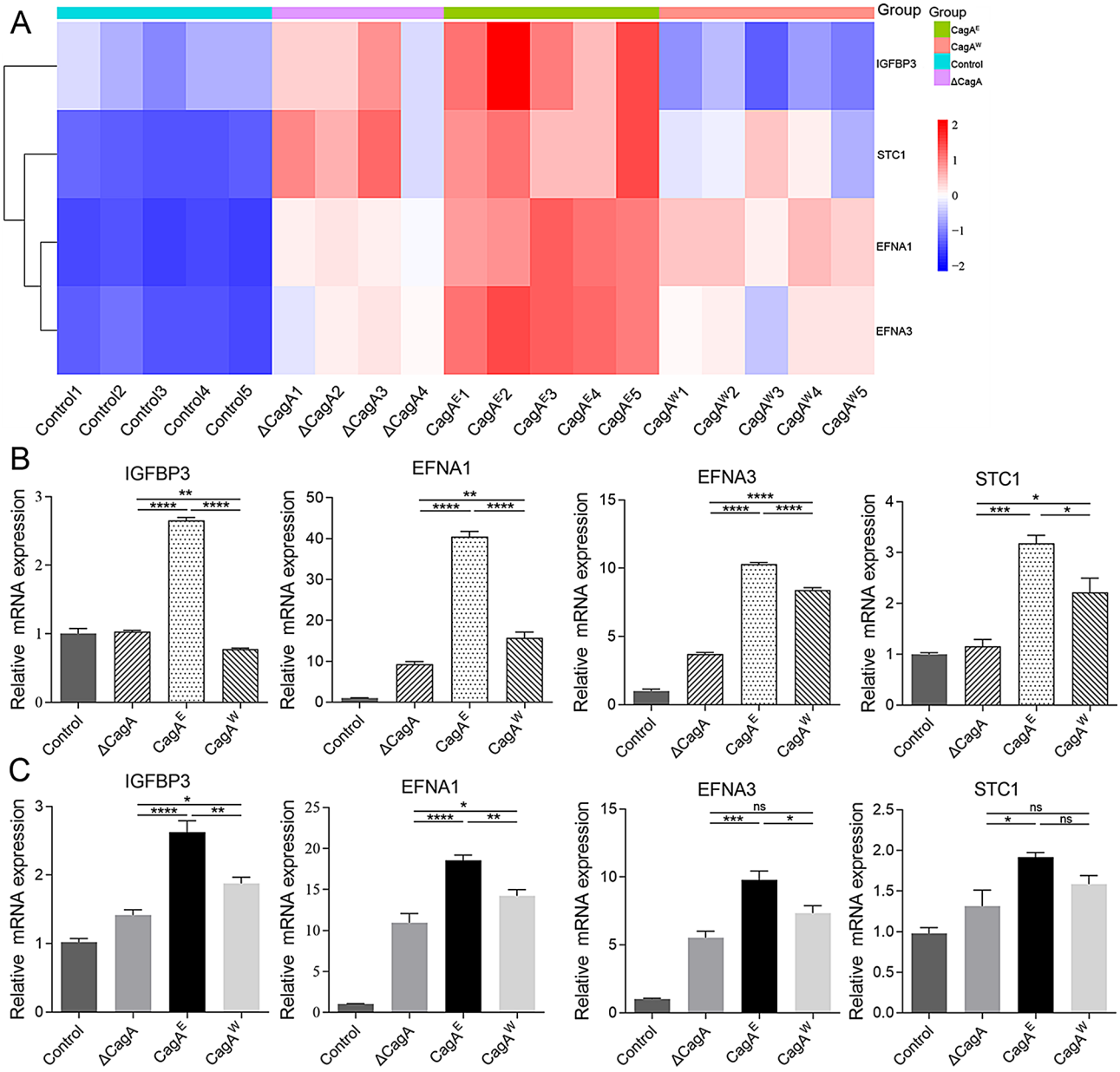

Fig. 5 Validation of the significantly differentially expressed genes associated with Hypoxia. (**A**) The heatmap shows the significantly upregulated mRNAs. Transcript levels assessment of genes in infected GES-1 cells (**B**) and mouse gastric organoids (**C**) was performed by qRT-PCR. GAPDH was selected as an internal control for relative quantification. ns, no significance, *$P < 0.05$, **$P < 0.01$, ***$P < 0.001$ and ****$P < 0.0001$

stronger effect on ERK pathway activation than $CagA^W$ [56]. Hayashi et al. demonstrated $CagA^E$ binds more tightly to SHP2, leading to greater activation of SHP2 and enhanced pathogenicity [32]. These studies suggest that the differences in intracellular signal regulation between $CagA^E$ and $CagA^W$ may underlie the stronger carcinogenicity of $CagA^E$.

In this study, we performed transcriptomic analysis to investigate the intracellular signaling profile of CagA. Since CagA acts quickly upon delivery into host cells, using a "hit-and-run" strategy to trigger carcinogenesis [58], we selected a 4-hour post-infection time point to capture early signaling changes. Transcriptomic analysis revealed that *H. pylori* infection predominantly affects the signaling pathway related to TNF-α via NF-κB, hypoxia, inflammatory response, IFN-γ response, IL-6/JAK/STAT3 signaling, allograft rejection, IL2-STAT5 signaling, and DNA damage responses. Most of these biological processes have been previously linked to *H. pylori* infection [34–36].

CagA's activity was particularly reflected in the upregulation of TNF-α via NF-κB, inflammatory response, and

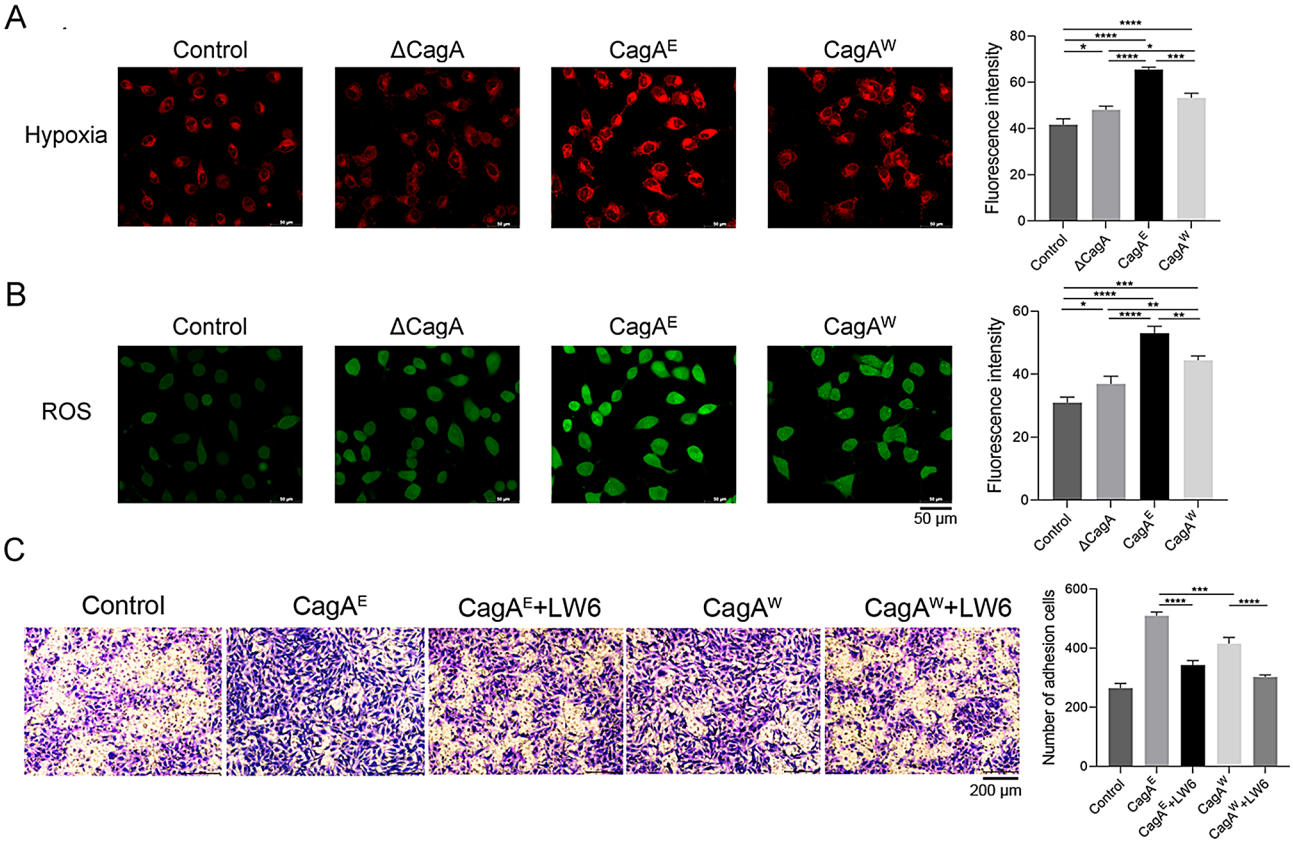

Fig. 6 Hypoxia analysis in GES-1 cells infected with *H. pylori*. (**A**) hypoxia and (**B**) ROS detection by ROS-ID hypoxia/oxidative stress detection kit. Red fluorescence indicates hypoxia level. Green fluorescence represents the degree of ROS production. (**C**) Cell migration detection of infected GES-1 cells with treatment of hypoxia inhibitor LW6. *$P < 0.05$, **$P < 0.01$, ***$P < 0.001$ and ****$P < 0.0001$

IFN-γ signaling, with CagA^E showing a more pronounced enrichment than CagA^W. This indicates that CagA^E is more potent in inducing inflammation and immune responses. Numerous studies have reported the association between CagA and inflammation [59, 60], particularly the activation of NF-κB by *H. pylori* infection, which leads to increased expression of TNF, CXCL8, and IL-8 secretion [61, 62]. Our RT-qPCR and ELISA results confirmed that CagA^E upregulates the expression of these inflammatory genes and promotes IL-8 secretion more effectively than CagA^W. Inflammation triggered by the NF-κB pathway is a key driver of CagA-induced gastric carcinogenesis [63]. Therefore, it is likely that CagA^E's stronger induction of inflammation contributes to its greater carcinogenicity.

Abnormal immune responses also play a critical role in the *H. pylori*-related gastric pathology. IFN-γ is a cytokine that modulates immune responses [64] and is highly expressed in *H. pylori*-infected gastric mucosa levels [65]. Our findings suggest that CagA^E has a stronger regulatory effect on IFN-γ signaling, although further studies are needed to clarify the mechanisms involved.

Hypoxia is directly related to tumor proliferation, migration, and invasion in GC [54, 66]. In this study, hypoxia-related genes such as IGFBP3, STC1, EFNA1, and EFNA3 were upregulated in response to CagA^E, and these genes are known to influence the tumor immune microenvironment and predict gastric cancer prognosis [67]. Although, research on *H. pylori* has been shown to upregulate Hif-1α, which is associated with increased invasion, metastasis, and reduced survival in gastric cancer patients [68, 69]. The relationship between CagA and hypoxia has not been well studied. Noto et al. recently reported that HIF-1α mitigates *H. pylori*-induced gastric injury by attenuating *cag*-mediated virulence and host inflammatory responses, suggesting a connection between the HIF-1α pathway and the *cag* pathogenicity island [70]. Our data show that CagA^E induces more severe hypoxia and higher ROS production in infected GES-1 cells, and blocking HIF-1α reduced cell migration, supporting the idea that CagA^E promotes cell migration by inducing hypoxia during *H. pylori* infection.

Additionally, our results indicated that CagA^E significantly upregulates genes involved in the UV response, a pathway associated with DNA damage [71]. *H. pylori* has been shown to cause extensive DNA double-strand breaks during GC development [72], and CagA contributes to genomic instability by disrupting the balance

between DNA damage and repair [73]. Our findings suggest that $CagA^{E}$ induces more severe DNA damage than $CagA^{W}$, but further studies are needed to confirm this. We also found that the oncogenic KRAS pathway was enriched in the $CagA^{E}$ group. KRAS signaling has been implicated in gastric cancer progression [74]. For example, Yin et al. reported that abnormal activation of KRAS signaling was triggered in high-risk GC patients [75], while Yoon et al. demonstrated that KRAS activation in gastric adenocarcinoma cells stimulates EMT, promoting migration and invasion [76]. Yet, the connection between CagA and KRAS activation has not yet been established and warrants further investigation.

In conclusion, our analysis demonstrates that $CagA^{E}$ exerts stronger regulatory effects on intracellular signaling pathways than $CagA^{W}$, particularly in inducing hypoxia. These findings help explain the higher oncogenic potential of $CagA^{E}$ in *H. pylori*-induced carcinogenesis.

Supplementary Information

The online version contains supplementary material available at https://doi.org/10.1186/s12866-024-03619-4.

Supplementary Material 1

Supplementary Material 2

Supplementary Material 3

Supplementary Material 4

Supplementary Material 5

Supplementary Material 6

Supplementary Material 7

Acknowledgements
We thank Bullet Edits Limited for the linguistic editing and proofreading of the manuscript.

Author contributions
Conceive and design the experiments: Xiaofei Ji and Huilin Zhao; Perform the experiments: Hao Wu, Xiaofei Ji, Zekun Sun, Jianhui Zhang, Shuzhen Liu, Xinying Cao, Ying Zhang, Boqing Li, Jiankai Feng, Huilin Zhao; Writing the paper: Xiaofei Ji, Hao Wu, Zekun Sun and Huilin Zhao; Revising the paper: Huilin Zhao and Xiaofei Ji; All authors approved the final manuscript.

Funding
This work was supported by Science and Technology Support Plan for Youth Innovation of Colleges and Universities of Shandong Province (2020KJK006) and Natural Science Foundation of Shandong Province (ZR2023MH101, ZR2020MH297).

Data availability
The RNA-Seq data has been uploaded to the NCBI-SRA with accession number PRJNA1070825.

Declarations

Ethical approval
The animal experiments were approved by the Animal Ethics Committee of Binzhou Medical University (Approval number: 2021-010).

Consent for publication
Not applicable.

Competing interests
The authors declare no competing interests.

Received: 21 March 2024 / Accepted: 4 November 2024
Published online: 11 November 2024

References

1. Fakharian F, Asgari B, Nabavi-Rad A, Sadeghi A, Soleimani N, Yadegar A, et al. The interplay between Helicobacter pylori and the gut microbiota: an emerging driver influencing the immune system homeostasis and gastric carcinogenesis. Front Cell Infect Microbiol. 2022;12:953718. https://doi.org/10.3389/fcimb.2022.953718.
2. Xu W, Xu L, Xu C. Relationship between Helicobacter pylori infection and gastrointestinal microecology. Front Cell Infect Microbiol. 2022;12:938608. https://doi.org/10.3389/fcimb.2022.938608.
3. Muzaheed. Helicobacter pylori Oncogenicity: mechanism, Prevention, and risk factors. Sci World J. 2020;2020:3018326. https://doi.org/10.1155/2020/3018326.
4. Nejati S, Karkhah A, Darvish H, Validi M, Ebrahimpour S, Nouri HR. Influence of Helicobacter pylori virulence factors CagA and VacA on pathogenesis of gastrointestinal disorders. Microb Pathog. 2018;117:43–8. https://doi.org/10.1016/j.micpath.2018.02.016.
5. Reshetnyak VI, Burmistrov AI, Maev IV. Helicobacter pylori: Commensal, symbiont or pathogen? World J Gastroenterol. 2021;27(7):545–60. https://doi.org/10.3748/wjg.v27.i7.545.
6. Chmiela M, Kupcinskas J, Review. Pathogenesis of Helicobacter pylori infection. Helicobacter. 2019;24 Suppl 1(Suppl Suppl 1):e12638; https://doi.org/10.1111/hel.12638
7. Cover TL, Lacy DB, Ohi MD. The Helicobacter pylori Cag type IV Secretion System. Trends Microbiol. 2020;28(8):682–95. https://doi.org/10.1016/j.tim.2020.02.004.
8. Takahashi-Kanemitsu A, Knight CT, Hatakeyama M. Molecular anatomy and pathogenic actions of Helicobacter pylori CagA that underpin gastric carcinogenesis. Cell Mol Immunol. 2020;17(1):50–63. https://doi.org/10.1038/s41423-019-0339-5.
9. Blaser MJ, Perez-Perez GI, Kleanthous H, Cover TL, Peek RM, Chyou PH, et al. Infection with Helicobacter pylori strains possessing cagA is associated with an increased risk of developing adenocarcinoma of the stomach. Cancer Res. 1995;55(10):2111–5.
10. Parsonnet J, Friedman GD, Orentreich N, Vogelman H. Risk for gastric cancer in people with CagA positive or CagA negative Helicobacter pylori infection. Gut. 1997;40(3):297–301. https://doi.org/10.1136/gut.40.3.297.
11. Hayashi T, Senda M, Morohashi H, Higashi H, Horio M, Kashiba Y, et al. Tertiary structure-function analysis reveals the pathogenic signaling potentiation mechanism of Helicobacter pylori oncogenic effector CagA. Cell Host Microbe. 2012;12(1):20–33. https://doi.org/10.1016/j.chom.2012.05.010.
12. Hatakeyama M. Oncogenic mechanisms of the Helicobacter pylori CagA protein. Nat Rev Cancer. 2004;4(9):688–94. https://doi.org/10.1038/nrc1433.
13. Hatakeyama M. Helicobacter pylori causes gastric cancer by hijacking cell growth signaling. Discov Med. 2004;4(24):476–81.
14. Hatakeyama M. Anthropological and clinical implications for the structural diversity of the Helicobacter pylori CagA oncoprotein. Cancer Sci. 2011;102(1):36–43. https://doi.org/10.1111/j.1349-7006.2010.01743.x.
15. Hatakeyama M, Higashi H. Helicobacter pylori CagA: a new paradigm for bacterial carcinogenesis. Cancer Sci. 2005;96(12):835–43. https://doi.org/10.1111/j.1349-7006.2005.00130.x.
16. Higashi H, Tsutsumi R, Fujita A, Yamazaki S, Asaka M, Azuma T, et al. Biological activity of the Helicobacter pylori virulence factor CagA is determined by variation in the tyrosine phosphorylation sites. Proc Natl Acad Sci U S A. 2002;99(22):14428–33. https://doi.org/10.1073/pnas.222375399.
17. Yamaoka Y. Mechanisms of disease: Helicobacter pylori virulence factors. Nat Rev Gastroenterol Hepatol. 2010;7(11):629–41. https://doi.org/10.1038/nrgastro.2010.154.
18. Jones KR, Joo YM, Jang S, Yoo YJ, Lee HS, Chung IS, et al. Polymorphism in the CagA EPIYA motif impacts development of gastric cancer. J Clin Microbiol. 2009;47(4):959–68. https://doi.org/10.1128/jcm.02330-08.

19. Yuan XY, Yan JJ, Yang YC, Wu CM, Hu Y, Geng JL. Helicobacter pylori with East Asian-type cagPAI genes is more virulent than strains with western-type in some cagPAI genes. Braz J Microbiol. 2017;48(2):218–24. https://doi.org/10.1016/j.bjm.2016.12.004.
20. Miura M, Ohnishi N, Tanaka S, Yanagiya K, Hatakeyama M. Differential oncogenic potential of geographically distinct Helicobacter pylori CagA isoforms in mice. Int J Cancer. 2009;125(11):2497–504. https://doi.org/10.1002/ijc.24740.
21. Argent RH, Hale JL, El-Omar EM, Atherton JC. Differences in Helicobacter pylori CagA tyrosine phosphorylation motif patterns between western and east Asian strains, and influences on interleukin-8 secretion. J Med Microbiol. 2008;57(Pt 9):1062–7. https://doi.org/10.1099/jmm.0.2008/001818-0.
22. Bridge DR, Blum FC, Jang S, Kim J, Cha JH, Merrell DS. Creation and initial characterization of isogenic Helicobacter pylori CagA EPIYA variants reveals Differential activation of host cell signaling pathways. Sci Rep. 2017;7. https://doi.org/10.1038/s41598-017-11382-y.
23. Freire de Melo F, Marques HS, Rocha Pinheiro SL, Lemos FFB, Silva Luz M, Nayara Teixeira K, et al. Influence of Helicobacter pylori oncoprotein CagA in gastric cancer: a critical-reflective analysis. World J Clin Oncol. 2022;13(11):866–79. https://doi.org/10.5306/wjco.v13.i11.866.
24. Odenbreit S, Püls J, Sedlmaier B, Gerland E, Fischer W, Haas R. Translocation of Helicobacter pylori CagA into gastric epithelial cells by type IV secretion. Science. 2000;287(5457):1497–500. https://doi.org/10.1126/science.287.5457.1497.
25. Mueller D, Tegtmeyer N, Brandt S, Yamaoka Y, De Poire E, Sgouras D, et al. c-Src and c-Abl kinases control hierarchic phosphorylation and function of the CagA effector protein in western and east Asian Helicobacter pylori strains. J Clin Invest. 2012;122(4):1553–66. https://doi.org/10.1172/jci61143.
26. Murata-Kamiya N, Kikuchi K, Hayashi T, Higashi H, Hatakeyama M. Helicobacter pylori exploits host membrane phosphatidylserine for delivery, localization, and pathophysiological action of the CagA oncoprotein. Cell Host Microbe. 2010;7(5):399–411. https://doi.org/10.1016/j.chom.2010.04.005.
27. Selbach M, Moese S, Hauck CR, Meyer TF, Backert S. Src is the kinase of the Helicobacter pylori CagA protein in vitro and in vivo. J Biol Chem. 2002;277(9):6775–8. https://doi.org/10.1074/jbc.C100754200.
28. Higashi H, Tsutsumi R, Muto S, Sugiyama T, Azuma T, Asaka M, et al. SHP-2 tyrosine phosphatase as an intracellular target of Helicobacter pylori CagA protein. Science. 2002;295(5555):683–6. https://doi.org/10.1126/science.1067147.
29. Mimuro H, Suzuki T, Tanaka J, Asahi M, Haas R, Sasakawa C. Grb2 is a key mediator of Helicobacter pylori CagA protein activities. Mol Cell. 2002;10(4):745–55. https://doi.org/10.1016/s1097-2765(02)00681-0.
30. Selbach M, Paul FE, Brandt S, Guye P, Daumke O, Backert S, et al. Host cell interactome of tyrosine-phosphorylated bacterial proteins. Cell Host Microbe. 2009;5(4):397–403. https://doi.org/10.1016/j.chom.2009.03.004.
31. Tegtmeyer N, Neddermann M, Asche CI, Backert S. Subversion of host kinases: a key network in cellular signaling hijacked by Helicobacter pylori CagA. Mol Microbiol. 2017;105(3):358–72. https://doi.org/10.1111/mmi.13707.
32. Hayashi T, Senda M, Suzuki N, Nishikawa H, Ben C, Tang C, et al. Differential mechanisms for SHP2 binding and activation are exploited by geographically distinct Helicobacter pylori CagA Oncoproteins. Cell Rep. 2017;20(12):2876–90. https://doi.org/10.1016/j.celrep.2017.08.080.
33. Chen D, Li C, Zhao Y, Zhou J, Wang Q, Xie Y. Bioinformatics analysis for the identification of differentially expressed genes and related signaling pathways in H. pylori-CagA transfected gastric cancer cells. PeerJ. 2021;9:e11203. https://doi.org/10.7717/peerj.11203.
34. Chen Z, Chen H, Yu L, Xin H, Kong J, Bai Y, et al. Bioinformatic identification of key pathways, hub genes, and microbiota for therapeutic intervention in Helicobacter pylori infection. J Cell Physiol. 2021;236(2):1158–83. https://doi.org/10.1002/jcp.29925.
35. Li N, Ouyang Y, Chen S, Peng C, He C, Hong J, et al. Integrative Analysis of Differential lncRNA/mRNA expression profiling in Helicobacter pylori infection-Associated gastric carcinogenesis. Front Microbiol. 2020;11:880. https://doi.org/10.3389/fmicb.2020.00880.
36. Zhu H, Wang Q, Yao Y, Fang J, Sun F, Ni Y, et al. Microarray analysis of long non-coding RNA expression profiles in human gastric cells and tissues with Helicobacter pylori Infection. BMC Med Genomics. 2015;8:84. https://doi.org/10.1186/s12920-015-0159-0.
37. Ji X, Zhao H, Zhang Y, Chen X, Li J, Li B. Construction of Novel plasmid vectors for gene knockout in Helicobacter pylori. Curr Microbiol. 2016;73(6):897–903. https://doi.org/10.1007/s00284-016-1140-7.
38. Mahe MM, Aihara E, Schumacher MA, Zavros Y, Montrose MH, Helmrath MA, et al. Establishment of gastrointestinal epithelial organoids. Curr Protoc Mouse Biol. 2013;3(4):217–40. https://doi.org/10.1002/9780470942390.mo130179.
39. Schumacher MA, Aihara E, Feng R, Engevik A, Shroyer NF, Ottemann KM, et al. The use of murine-derived fundic organoids in studies of gastric physiology. J Physiol. 2015;593(8):1809–27. https://doi.org/10.1113/jphysiol.2014.283028.
40. Teal E, Steele NG, Chakrabarti J, Holokai L, Zavros Y. Mouse- and human-derived primary gastric epithelial monolayer culture for the study of regeneration. J Vis Exp. 2018;13510.3791/57435.
41. Vallone VF, Leprovots M, Vassart G, Garcia MI. Ex vivo culture of adult mouse antral glands. Bio Protoc. 2017;7(1):e2088. https://doi.org/10.21769/BioProtoc.2088.
42. Schlaermann P, Toelle B, Berger H, Schmidt SC, Glanemann M, Ordemann J, et al. A novel human gastric primary cell culture system for modelling Helicobacter pylori infection in vitro. Gut. 2016;65(2):202–13. https://doi.org/10.1136/gutjnl-2014-307949.
43. Chen S, Zhou Y, Chen Y, Gu J. Fastp: an ultra-fast all-in-one FASTQ preprocessor. Bioinformatics. 2018;34(17):i884–90. https://doi.org/10.1093/bioinformatics/bty560.
44. Liao Y, Smyth GK, Shi W. featureCounts: an efficient general purpose program for assigning sequence reads to genomic features. Bioinformatics. 2014;30(7):923–30. https://doi.org/10.1093/bioinformatics/btt656.
45. Love MI, Huber W, Anders S. Moderated estimation of Fold change and dispersion for RNA-seq data with DESeq2. Genome Biol. 2014;15(12):550. https://doi.org/10.1186/s13059-014-0550-8.
46. Lin SM, Du P, Huber W, Kibbe WA. Model-based variance-stabilizing transformation for Illumina microarray data. Nucleic Acids Res. 2008;36(2):e11. https://doi.org/10.1093/nar/gkm1075.
47. Subramanian A, Tamayo P, Mootha VK, Mukherjee S, Ebert BL, Gillette MA, et al. Gene set enrichment analysis: a knowledge-based approach for interpreting genome-wide expression profiles. Proc Natl Acad Sci U S A. 2005;102(43):15545–50. https://doi.org/10.1073/pnas.0506580102.
48. Wu T, Hu E, Xu S, Chen M, Guo P, Dai Z, et al. clusterProfiler 4.0: a universal enrichment tool for interpreting omics data. Innov (Camb). 2021;2(3):100141. https://doi.org/10.1016/j.xinn.2021.100141.
49. Livak KJ, Schmittgen TD. Analysis of relative gene expression data using real-time quantitative PCR and the 2(-Delta Delta C(T)) method. Methods. 2001;25(4):402–8. https://doi.org/10.1006/meth.2001.1262.
50. Rao X, Huang X, Zhou Z, Lin X. An improvement of the 2^(-delta delta CT) method for quantitative real-time polymerase chain reaction data analysis. Biostat Bioinforma Biomath. 2013;3(3):71–85.
51. Lu H, Murata-Kamiya N, Saito Y, Hatakeyama M. Role of partitioning-defective 1/microtubule affinity-regulating kinases in the morphogenetic activity of Helicobacter pylori CagA. J Biol Chem. 2009;284(34):23024–36. https://doi.org/10.1074/jbc.M109.001008.
52. Lu HS, Saito Y, Umeda M, Murata-Kamiya N, Zhang HM, Higashi H, et al. Structural and functional diversity in the PAR1b/MARK2-binding region of Helicobacter pylori CagA. Cancer Sci. 2008;99(10):2004–11. https://doi.org/10.1111/j.1349-7006.2008.00950.x.
53. Ferreira RM, Pinto-Ribeiro I, Wen X, Marcos-Pinto R, Dinis-Ribeiro M, Carneiro F, et al. Helicobacter pylori cagA promoter region sequences influence CagA expression and interleukin 8 secretion. J Infect Dis. 2016;213(4):669–73. https://doi.org/10.1093/infdis/jiv467.
54. Pei JP, Zhang CD, Yusupu M, Zhang C, Dai DQ. Screening and validation of the Hypoxia-Related signature of evaluating Tumor Immune Microenvironment and Predicting Prognosis in Gastric Cancer. Front Immunol. 2021;12:705511. https://doi.org/10.3389/fimmu.2021.705511.
55. Xu C, Chen Y, Chen X, Wang F. Effects of different types of Helicobacter pylori on the gap junction intercellular communication in GES-1 cells. Zhong Nan Da Xue Xue Bao Yi Xue Ban. 2011;36(4):294–300. https://doi.org/10.3969/j.issn.1672-7347.2011.04.003.
56. Fu HY, Asahi K, Hayashi Y, Eguchi H, Murata H, Tsujii M, et al. East asian-type Helicobacter pylori cytotoxin-associated gene A protein has a more significant effect on growth of rat gastric mucosal cells than the western type. J Gastroenterol Hepatol. 2007;22(3):355–62. https://doi.org/10.1111/j.1440-1746.2006.04531.x.
57. Backert S, Tegtmeyer N, Type IV. Secretion and Signal Transduction of Helicobacter pylori CagA through interactions with Host Cell Receptors. Toxins. 2017;9(4). https://doi.org/10.3390/toxins9040115.

58. Hatakeyama M. Structure and function of Helicobacter pylori CagA, the first-identified bacterial protein involved in human cancer. Proc Jpn Acad Ser B Phys Biol Sci. 2017;93(4):196–219. https://doi.org/10.2183/pjab.93.013.
59. Lamb A, Chen LF. Role of the Helicobacter pylori-induced inflammatory response in the development of gastric cancer. J Cell Biochem. 2013;114(3):491–7. https://doi.org/10.1002/jcb.24389.
60. Săsăran MO, Meliț LE, Dobru ED. MicroRNA modulation of Host Immune Response and inflammation triggered by Helicobacter pylori. Int J Mol Sci. 2021;22(3). https://doi.org/10.3390/ijms22031406.
61. Lamb A, Chen LF. The many roads traveled by *Helicobacter pylori* to NFκB activation. Gut Microbes. 2010;1(2):109–13. https://doi.org/10.4161/gmic.1.2.11587.
62. Tang CL, Hao B, Zhang GX, Shi RH, Cheng WF. *Helicobacter pylori* tumor necrosis factor-α inducing protein promotes cytokine expression via nuclear factor-κB. World J Gastroenterol. 2013;19(3):399–403. https://doi.org/10.3748/wjg.v19.i3.399.
63. Yang F, Xu Y, Liu C, Ma C, Zou S, Xu X, et al. NF-κB/miR-223-3p/ARID1A axis is involved in *Helicobacter pylori* CagA-induced gastric carcinogenesis and progression. Cell Death Dis. 2018;9(1):12. https://doi.org/10.1038/s41419-017-0020-9.
64. Schroder K, Hertzog PJ, Ravasi T, Hume DA. Interferon-gamma: an overview of signals, mechanisms and functions. J Leukoc Biol. 2004;75(2):163–89. https://doi.org/10.1189/jlb.0603252.
65. Zhao Y, Zhou Y, Sun Y, Yu A, Yu H, Li W, et al. Virulence factor cytotoxin-associated gene A in *Helicobacter pylori* is downregulated by interferon-γ in vitro. FEMS Immunol Med Microbiol. 2011;61(1):76–83. https://doi.org/10.1111/j.1574-695X.2010.00750.x.
66. Bhandari V, Hoey C, Liu LY, Lalonde E, Ray J, Livingstone J, et al. Molecular landmarks of tumor hypoxia across cancer types. Nat Genet. 2019;51(2):308–. https://doi.org/10.1038/s41588-018-0318-2.
67. Zhou K, Cai C, Ding G, He Y, Hu D. A signature of six-hypoxia-related genes to evaluate the tumor immune microenvironment and predict prognosis in gastric cancer. BMC Med Genomics. 2022;15(1):261. https://doi.org/10.1186/s12920-022-01411-9.
68. Canales J, Valenzuela M, Bravo J, Cerda-Opazo P, Jorquera C, Toledo H, et al. *Helicobacter pylori* Induced Phosphatidylinositol-3-OH Kinaseactivationvincreasesreases Hypoxia Inducible Factor-promoterlosse LocyclinCyclin D1 and cell1cycle arrestArrehuman gastricacells Cells. Front Cell Infect Microbiol. 2017;7:92. https://doi.org/10.3389/fcimb.2017.00092.
69. Ozcan G. The hypoxia-inducible factor-1α in stemness and resistance to chemotherapy in gastric cancer: future directions for therapeutic targeting. Front Cell Dev Biol. 2023;11:1082057. https://doi.org/10.3389/fcell.2023.1082057.
70. Noto JM, Piazuelo MB, Romero-Gallo J, Delgado AG, Suarez G, Akritidou K, et al. Targeting hypoxia-inducible factor-1 alpha suppresses Helicobacter pylori-induced gastric injury via attenuation of both cag-mediated microbial virulence and proinflammatory host responses. Gut Microbes. 2023;15(2):2263936. https://doi.org/10.1080/19490976.2023.2263936.
71. Liberzon A, Birger C, Thorvaldsdóttir H, Ghandi M, Mesirov JP, Tamayo P. The Molecular signatures database (MSigDB) hallmark gene set collection. Cell Syst. 2015;1(6):417–25. https://doi.org/10.1016/j.cels.2015.12.004.
72. Murata-Kamiya N, Hatakeyama M. Helicobacter pylori-induced DNA double-stranded break in the development of gastric cancer. Cancer Sci. 2022;113(6):1909–18. https://doi.org/10.1111/cas.15357.
73. Kontizas E, Tastsoglou S, Karamitros T, Karayiannis Y, Kollia P, Hatzigeorgiou AG, et al. Impact of Helicobacter pylori infection and its major virulence factor CagA on DNA damage repair. Microorganisms. 2020;8(12). https://doi.org/10.3390/microorganisms8122007.
74. Balakrishnan K, Ganesan K. Identification of oncogenic signaling pathways associated with the dimorphic metabolic dysregulations in gastric cancer subtypes. Med Oncol. 2022;39(9). https://doi.org/10.1007/s12032-022-01717-9.
75. Yin Z, Qiao Y, Shi J, Bu L, Ao L, Tang W, et al. Identification of Costimulatory Molecule-related lncRNAs Associated with gastric carcinoma progression: evidence from Bioinformatics Analysis and Cell experiments. Front Genet. 2022;13:950222. https://doi.org/10.3389/fgene.2022.950222.
76. Yoon C, Till J, Cho SJ, Chang KK, Lin JX, Huang CM, et al. KRAS activation in gastric adenocarcinoma stimulates epithelial-to-mesenchymal transition to Cancer Stem-Like cells and promotes metastasis. Mol Cancer Res. 2019;17(9):1945–57. https://doi.org/10.1158/1541-7786.Mcr-19-0077.

Publisher's note